[12]R. H. Bube, *Photoconductivity of Solids* (Wiley, New York, 1960).
[13]R. Schubert and K. W. Böer, J. Phys. Chem. Solids **32,** 71 (1971).
[14]Homogeneous doping is also indicated from the observed linear dependence of the width of a high-field domain on the applied voltage.
[15]J. Fassbender, Z. Phys. **145,** 310 (1953).
[16]G. A. Dussel and K. W. Böer, Phys. Status Solidi **39,** 375 (1970).

PHYSICAL REVIEW B VOLUME 7, NUMBER 4 15 FEBRUARY 1973

Photoconductor-Metal Contact at Higher Densities*

G. A. Dussel† and K. W. Böer
Department of Physics, University of Delaware, Newark, Delaware 19711

R. J. Stirn
Jet Propulsion Laboratory, Pasadena, California 91103

(Received 9 June 1971)

The formation of space charge in the barrier region is discussed. This region extends to $x_0 \simeq 200$ Å $+ 2\lambda$ (λ is the mean free path of majority carriers). The conventional transport equation can be used only for $x > x_0$, and the carrier density at x_0 represents a boundary condition for the bulk. Its change as a function of applied voltage, temperature, and light intensity in photoconducting CdS is discussed. The time dependence of the space-charge formation in the region $0 < x < x_0$ is analyzed. It is shown under which conditions the individuality of the metal contact is observable.

I. INTRODUCTION

In the preceding paper[1] we have shown that at higher current densities, a model using a simple carrier transport and Poisson equation to explain the behavior in the barrier near a "blocking" cathode breaks down. This situation can be reached with photoconducting CdS and with current densities greater than $\sim 10^{-7}$ A/cm^2. It was suggested[1] that tunneling through the barrier is the major effect to provide current continuity. This is in agreement with the suggestions made earlier by several authors (for a summary, see Ref. 2) and by itself does not seem to necessitate a careful new study. However, the recently developed method of high-field domains[3] made it possible to determine unambiguously the maximum field F_{II} starting at a distance x_0 from the electrode interface. The distance x_0 is that distance from the interface beyond which the simple transport equation

$$j = e\mu(F)\, n(F)\, F - \mu kT \frac{dn}{dx} \quad , \tag{1}$$

and Poisson equation

$$\frac{dF}{dx} = \frac{e}{\epsilon\epsilon_0}\, \rho(n, F) \tag{2}$$

are valid. This maximum field F_{II} is too low and x_0 is too small to accommodate enough space charge in a slab $0 < x < x_0$ in lightly doped photoconductors ($N_D < 10^{17}$ cm^{-3}) to reach critical fields necessary for sufficient tunneling. We therefore had to assume that additional donors of $\sim 10^{18}$ cm^{-3} are always present in CdS at an energy not accessible to conventional detection methods, since no other known process but tunneling could account for the observed current densities. We have investigated[1] the stationary and kinetic behavior of the current across a barrier caused by different metal-CdS combinations, and in this paper will give a more detailed analysis of the process taking place in the thin (of the order of a few mean free paths of majority carriers) barrier layer ($0 < x < x_0$).

II. IMAGE FORCE REGION

The potential distribution in the barrier region is determined by four factors: (i) the image forces, (ii) the difference of work functions between the metal and the photoconductor, (iii) the space-charge distribution determined by the carrier kinetics, and (iv) the external field. The image force of a carrier is attractive toward the metal and its potential is given by

$$V(x) = \frac{e}{16\,\pi\epsilon_0\epsilon_\infty x} \quad , \tag{3}$$

where ϵ_∞ is the optical dielectric constant and ϵ_0 is the permittivity of free space. This potential distribution is shown in Fig. 1 for electrons and holes. It should be pointed out that close to the photoconductor-metal interface there is no change in the band gap, as it appears from Fig. 1, because an image force is experienced by either an electron (both bands bend downward) or by a hole (both bands bend upward) if they are located close to the electrode. However, when an electron and a hole are closer together than their separation from the electrode, a dipole-dipole interaction re-

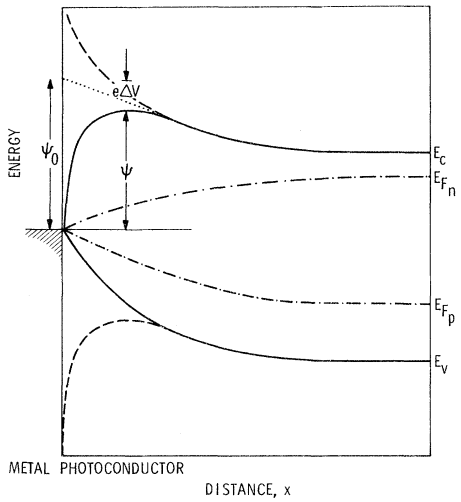

FIG. 1. Potential distribution in a photoconductor under illumination near a blocking contact (zero external field). E_{F_n} and E_{F_p} are the quasi-Fermi levels for electrons and holes, respectively. The solid curves are the relevant bands for electrons and holes (in the image force region).

places the monopole image potential [Eq. (1)] with considerably less effect on the bands. In moving parallel to the photoconductor-electrode interface, a valence-band electron sees a potential which is obviously highly perturbed, alternating between small areas in which the band bends upward or downward.

The region in which the image force has a marked influence on the electrical properties is very close to the photoconductor-electrode interface and extends not beyond a distance x_{00} at which the image force influence is of the order of kT, i.e., beyond

$$x_{00} = e^2/16\pi\epsilon_0\epsilon_\infty kT \ , \tag{4}$$

which is about 30 Å for CdS at room temperature. This model is valid for carrier densities below x_{00}^{-3}, i.e., below 3×10^{19} cm^{-3}. At higher carrier densities, carrier compensation is usually required[4] and the monopole image force region disappears. In the case investigated here, the carrier density is far below this critical value.

The fact that the image force is always attractive does not allow it to be helpful for storage of minority carriers necessary for lowering a barrier. To the contrary, it enhances the extraction of minority carriers from the entire barrier region.

On the other hand, the image force aids the majority-carrier transport across the barrier by reducing its height in an external field F_m by an amount

$$\Delta V = \frac{1}{2\sqrt{\pi}} \left(\frac{e}{\epsilon_0\epsilon_\infty} F_m\right)^{1/2} \tag{5}$$

Therefore, the height of the barrier is given by $\psi = \psi_0 - e\Delta V$, where ψ_0, the work function between the metal and photoconductor, can be determined by a number of methods in the zero-current limit (for a summary, see Ref. 5).

The experimental results given in Ref. 1 cannot be explained by a reduction in barrier height caused by the image force[6,7] since it would need a field F_m far in excess of 10^6 V/cm. Long before this field is reached, tunneling through the barrier would take over.

A marked lowering of the critical field for tunneling can occur when Coulomb attractive centers of sufficient density are available, as was recently shown by Parker and Mead.[8,9] This seems to be the case in CdS and we will therefore assume that this mechanism is responsible for tunneling through the barrier. (Conventional tunneling or thermally-assisted tunneling would require higher fields at the barrier, and therefore higher space-charge density.) In Fig. 2 a schematic comparison is shown for tunneling through a "clean" barrier (solid arrow) and through a barrier with a Coulomb-attractive trap (dashed arrow) with about the same total tunneling probability. For the typical current densities observed in Ref. 1, the tunneling field is of the order of 3×10^5 V/cm. This value will be used for the following analysis.

III. SPACE CHARGE IN THE BARRIER LAYER

A "blocking" contact on an n-type semiconductor is characterized by a positive space-charge region close to the cathode. The field increases toward the cathode following the Poisson equation [Eq. (2)]. This field must reach values of the tunneling field strength (3×10^5 V/cm) in order to produce the

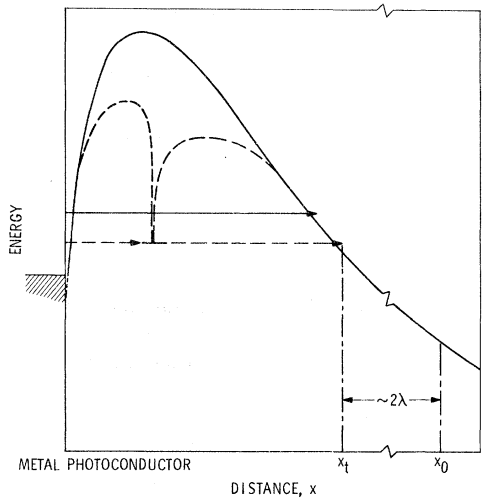

FIG. 2. Tunneling of electrons through a clean barrier (solid arrow) and through a barrier with a Coulomb attractive trap (dashed arrow).

observed current densities. This tunneling field is considerably larger than the observed field in the high-field domain, posing the problem of storing positive space charge in the barrier region with a layer density of $\rho\Delta x \simeq 3\times10^{12}$ cm^{-2}. Δx is the width of the layer starting at the location x_t of "emergence" of tunneling electrons and ending at the position x_0, where the simple transport equation (1) becomes valid (see Fig. 2).

The location x_t can be estimated as the thickness of the barrier at the Fermi level. For a barrier height of 0.6 eV and a tunneling field of 3×10^5 V/cm, x_t is 200 Å.

The location x_0 was defined in Ref. 1 for a simple model. For $x > x_0$ the parameters of the transport equation do not explicitly depend on the spacial coordinate. We will discuss this here in more detail for the two main parameters of the transport equation—the carrier density and the mobility.

The mobility is a local property if the potential changes by more than kT within a mean free path λ and as long as the carrier momentum distribution is tunneling influenced. The first condition determines a critical length x_1 given by

$$e[F(x_1-\lambda)-F(x_1)]\lambda = kT. \tag{6}$$

The second condition is more difficult to estimate. The momentum distribution of the carriers emerging after tunneling at the edge of the conduction band is anisotropic, essentially pancake-like with the large axis parallel to the electrode surface.[10,11] This anisotropy can amount to several kT at higher fields, necessitating a few scattering events for "thermalization."[12] We will therefore assume that such thermalization is reached at $x_2 = x_t + \zeta\lambda$ with $\zeta \simeq 2$.

The carrier density (more generally, the distribution of trapped and free charges) is a *local property* only as long as the energy distribution of free carriers is a local property. Otherwise, it is unambiguously determined by spacially independent parameters and the field. This is the case for $x \geq x_2$.

Therefore, the simple transport and Poisson equations [Eqs. (1) and (2)] are valid for $x > x_0$, with x_0 being the larger one of the distances x_1 or x_2. If the tunneling field and the space charge in Δx are known, the boundary condition at x_0 for Eqs. (1) and (2) can be determined.

The positive space charge in Δx must be stored as holes trapped below, but near, the Fermi level, since electron traps between the Fermi level and the electron quasi-Fermi level, which could be depleted by the field, are not numerous enough to provide the necessary charge.[13] Hole traps in the lower part of the band gap must be rejected as possible storage centers, since it is known that already at somewhat lower fields (F_{II}^*), these centers are depleted of holes by means of field-enhanced ionization.[14,15] Since in photoconductive CdS, the Fermi level is essentially pinned[16] near 0.8 eV below the conduction band, it is reasonable to assume that a level is located here with a density exceeding the density of the other known levels. Since this density exceeds the density of known impurities, it is suggested that these levels are caused by native defects. Single native defects which could be present in such high density are V_{Cd}, V_S, and Cd_i. The cadmium vacancy is usually associated with sensitizing centers leaving either Cd_i or V_S to cause the proposed donor level at 0.8 eV. Since no trap level of comparable density is observed in the range $0.8 < E_c - E_t < 0.2$ eV, one must assume that this level is singly charged (the doubly ionized level lies even deeper), and that major compensation by V_{Cd} does not occur since the Fermi level is not observed to drop markedly below the assumed position of the donor level.

However, from the high-field analysis we know that in the bulk of the crystal at fields larger than F_{II} (at the transition from F_{II} to F_{III}—as seen with anode-adjacent high-field domains[17]), instead of the positive space-charge layer, a negative space charge is formed. *We therefore must assume that the creation of the positive space charge near the cathode is intrinsically connected with its proximity to the barrier.* In the barrier layer for $x < x_2$, the recombination kinetics are indeed characteristically different from the bulk. The population of the centers assumed to be responsible for the space charge here is determined by the balance between capture and ionization. The ionization depends only on the field; hence, it should be the same near the electrode and in the bulk for an F_{III} transition. However, capture by Coulomb-attractive centers depends markedly[18] on the electron-energy distribution (field-enhanced ionization[14]) and is considerably smaller near the electrode than in the bulk—possibly because of the excess energy (with k vectors parallel to the electrode surface) that electrons retain after tunneling. This may cause the population of the centers near the electrode at ~0.8 eV to decrease,[14] producing the positive space charge as required.[19] This fact reinforces our choice of levels near 0.8 eV for explanation of the origin of the space charge, since a kinetic equilibrium as required above can only be influenced for levels with marked field-ionization probability. This is the case for Coulomb-attractive centers not too far below the Fermi level.[14]

An estimation of the space-charge distribution in the steady state can be made by equating the capture and emission rates, i.e.,

$$(j_n/e)\, q(F)\, (N_D - n_D) = \alpha(F)\, n_D\ , \tag{7}$$

where $q(F)$ and $\alpha(F)$ are the field-dependent cap-

ture cross section and ionization probability, respectively, with N_D the total density of donors at ~0.8 eV, and n_D the density of electrons in these donors. Using Poisson equation with $\rho = N_D - n_D$, one obtains

$$\frac{dF}{dx} = \frac{e}{\epsilon\epsilon_0} N_D \left(1 - \frac{j_n q(F)}{e\alpha(F) + j_n q(F)}\right) , \tag{8}$$

yielding a sufficient positive space charge for $N_D \gtrsim 10^{18}$ cm^{-3} and $q(F) < q(F_j)$, where

$$q(F_j) = e\alpha(F_j)/j_n . \tag{9}$$

Since $q(F)$ decreases and $\alpha(F)$ increases with F, one expects the donor levels to be filled for $F < F_j$ and to be essentially empty for the fields above F_j. In the bulk, one obtains[14] for $j \simeq 10^{-2}$ A/cm^2 (as observed in the high-field-domain range) a critical field $F_j \simeq 1.6 \times 10^5$ V/cm which is close to the observed F_{III} (see Fig. 6 in Ref. 1). Therefore, these deep donor levels (N_D) should be inactive in the bulk until field values of this order are reached. Indeed, below these values, negative space charge is experimentally observed (here compensating acceptors are depleted via field quenching, which by the same mechanism is already active at somewhat lower fields).

If $q(F)$ is decreased by a factor of 10 in the contact region because of the anisotropy of the electron energy distribution of the recombining electrons, the critical field for depletion of these donors is reduced to 70 kV/cm. Hence, a positive space charge is produced for $F > 70$ kV/cm as long as electrons with excessive energy from tunneling are available. With increasing x, however, thermalization of tunneling electrons increases, thus increasing F_j and causing the positive space-charge region to terminate rather abruptly.[1]

Since the field must decrease from $F(x_t)$ to F_{II} when thermalization is reached (at $\sim x_t + 2\lambda$), one estimates the density of donors as

$$F(x_t) - F_{II} \simeq F(x_t) = 2(e/\epsilon\epsilon_0)\rho\,\lambda . \tag{10}$$

With[9] $F(x_t) \geq 3 \times 10^5$ V/cm and $\lambda \simeq 200$ Å we obtain $\rho \simeq N_D \geq 4 \times 10^{17}$ cm^{-3}. Since $N_D > 10^{17}$ cm^{-3}, it follows[1] that Eq. (6) is not satisfied until the donors become markedly filled, hence, $x_1 \simeq x_2 = x_0 \simeq 600$ Å.

IV. BOUNDARY CONDITION FOR CRYSTAL BULK

For $x \geq x_0$, the Poisson and the simple transport equation determine the field and carrier distribution so that the field of direction[1] can advantageously be used used for an analysis. The solution curve is unambiguously selected by $n(x_0)$ and $F(x_0)$. In the high-field domain regime, this boundary condition represents a point in the close proximity of the singular point II for the case discussed above (see Fig. 3 of Ref. 1). This singular point can easily be obtained when the tunneling field $F(x_t)$ and the space charge in the region $x_t < x < x_0$ is known. The field decreases in $x_0 - x_t$ by

$$\Delta F = F(x_t) - F(x_0) = \frac{e}{\epsilon\epsilon_0} \int_{x_t}^{x_0} \rho(x)\,dx \simeq \frac{eN_D(x_0 - x_t)}{\epsilon\epsilon_0} . \tag{11}$$

The current as a function of the tunneling field $F(x_t)$ as calculated from the tunnel equation and as a function of $F(x_0)$ is given in Fig. 3. $j[F(x_0)]$ intersects the j-F characteristic calculated for a homogeneous field,

$$j_h = e\mu(F)\, n_1(F)\, F , \tag{12}$$

at the singular point II. Since $j[F(x_0)]$ is shifted from $j[F(x_t)]$ by an amount dependent on N_D [see Eq. (7)], the boundary point II depends on N_D as well as on $j[F(x_t)]$, i.e., on the barrier height. The solution (solid arrow) extends between the vicinity of singular points II and I and has domain character.

Since $j[F(x_t)]$ shifts toward higher fields with increasing barrier height, $j[F(x_0)]$ must also shift toward higher fields for the same CdS crystal (same N_D). Hence, the current must decrease and F_{II} must increase, as experimentally observed (Figs. 8 and 9 in Ref. 1).

On the other hand, for photoconductors with lower donor concentration, the $j[F(x_0)]$ curve [Fig. 3(a)] is closer to $j[F(x_t)]$ and may intersect j_h at fields above the field at its minimum. The solution will then squeeze below the minimum of j_h through the quasisingular point II* as indicated by the dashed arrow in Fig. 3.

The other extreme of a very high density of donors may be acheived without changing the bulk

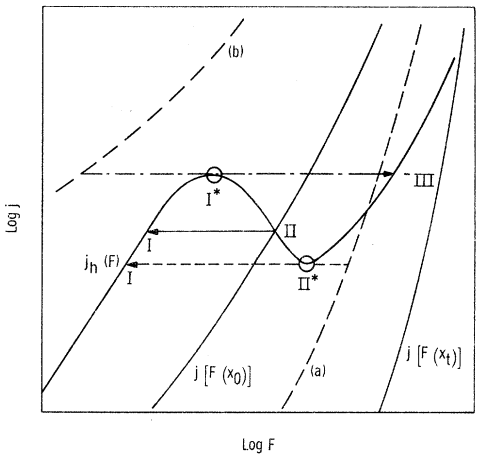

FIG. 3. Current density j_h calculated for homogeneous fields F; current density $j[F(x_t)]$ caused by tunneling assisted by Coulomb attractive centers; and current density $j[F(x_0)]$ as a function of the field at the position x_0 as defined in Sec. III. Curves (a) and (b) represent current densities $j[F(x_0)]$ for a crystal with lower and higher donor density, respectively.

properties by highly disordering a near-surface region (e.g., via a gas discharge[20]) before applying the electrode. Here $j[F(x_0)]$ is further separated from $j[F(x_t)]$ and, in Fig. 3, is represented by the dashed curve (b) indicating injecting behavior. In the domain regime the solution squeezes through the quasisingular point I* and reaches close to the singular point III (dash-dotted arrow), representing an anode-adjacent high-field domain in agreement with the experimental observation.[17]

V. DEPENDENCE ON OPTICAL EXCITATION AND TEMPERATURE

With increasing optical excitation rate (a), the currents $j[F(x_t)]$ and $j[F(x_0)]$ [curve pair (a) in Fig. 4] are not affected. However, $j_h(F) = e\mu n_1(a)F$ is shifted upward with increasing optical excitation as shown in Fig. 4 for a family of curves $j_h(F)$. The intersect of $j[F(x_0)]$ and $j_h(F)$ moves toward higher F with increasing a and one expects, therefore, an increase of F_{II} and of the current density in the domain regime with excitation density, as experimentally observed (Fig. 7 in Ref. 1).

For metal-CdS contacts with a low work function, the tunneling field is considerably lower, i.e., $j[F(x_t)]$ and $j[F(x_0)]$ [curve pair (b) in Fig. 4] are shifted toward lower fields. However, the critical field given by Eq. (9) and shown as $j_n(F)$ in Fig. 4 at which the production of positive space charge in the barrier region ceases, may be reached at $x = x_3$ with $x_3 < x_0$. Since the field cannot be reduced markedly below $F(x_3)$, the boundary field at x_0 is essentially $F(x_3)$. Since $j_n(F)$ is steeper than

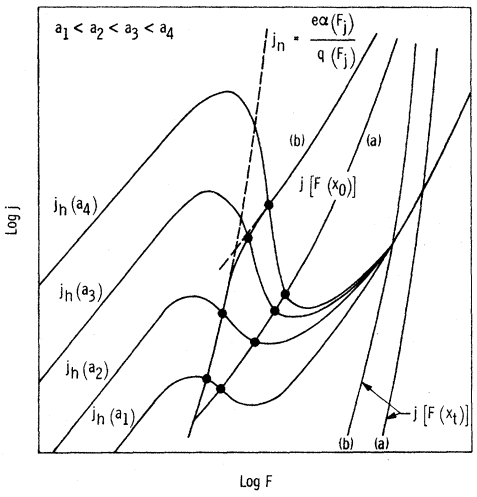

FIG. 4. $j_h(F)$ for different optical excitation densities a, and $j[F(x_t)]$, $j[F(x_0)]$ for larger [curve pair (a)] and smaller [(curve pair (b)] barrier heights for the same photoconductor. j_n is the limiting current density due to space-charge saturation via field-enhanced ionization [Eq. (9)].

$j[F(x_0)]$, one expects a smaller dependence of F_{II} on the optical excitation for less blocking contacts. This is also observed experimentally (Fig. 7 in Ref. 1).

The change of F_{II} and j with increasing temperature is less transparent since a number of effects compete here: (i) The current density j_h changes because of $n(T)$ and $\mu(T)$. (ii) The mean free path, hence x_0, decreases with increasing T. (iii) The critical field given by Eq. (9) decreases with increasing T.

Since λ and F_j given by Eq. (9) increases with decreasing T, one expects Eq. (9) to control the boundary condition for higher barriers at lower temperatures. In this case, the field F_{II} should increase with decreasing temperatures (see Fig. 5) as j_h shifts toward higher fields. A slight decrease in saturation current with decreasing temperature is expected (Fig. 5) in spite of an increase of j_h (caused by an increase in μ and n at lower temperatures because of reduction in scattering and of thermal quenching). This behavior agrees qualitatively with the experimental results [Figs. 7 and 8(c) of Ref. 1]. At temperatures below 200 °K however, the model used for field-enhanced ionization[12] must be refined, and a simple evaluation as given above is not sufficient.

VI. TIME-DEPENDENT BEHAVIOR

The transient behavior of the current after the applied voltage is switched [Figs. 9(a) and 9(b), Ref. 1] can be explained by an analysis of the field-aided redistribution of trapped and free carriers near the cathode. We will show this by discussing the particle current of the photoconductor near the cathode.

Before an external voltage is applied, the distribution of carriers is homogeneous in the bulk, and for a given optical excitation is sufficiently described by the two quasi-Fermi levels E_{F_n} and E_{F_p}. This homogeneous region extends to a distance of a few Debye screening lengths λ_D from the cathode, where

$$\lambda_D = (8\pi\epsilon\epsilon_0 kT/eN^+)^{1/2} . \tag{13}$$

This length is of the order of 10^{-5} cm for an assumed density of positively charged defects N^+ of about 10^{16} cm^{-3} (zero external field).

When an external voltage V_a is applied, initially a homogeneous external field $F_a = V_a/L$ is superimposed to the local field at each point of the crystal and a current starts to flow. However, since the density of electrons in the barrier region is smaller than in the bulk, the current in this region cannot be carried completely by drift in the external field. As a consequence, the field there must increase, yielding a displacement-current contribution $\epsilon\epsilon_0(\partial F/\partial t)$ in the barrier region. This

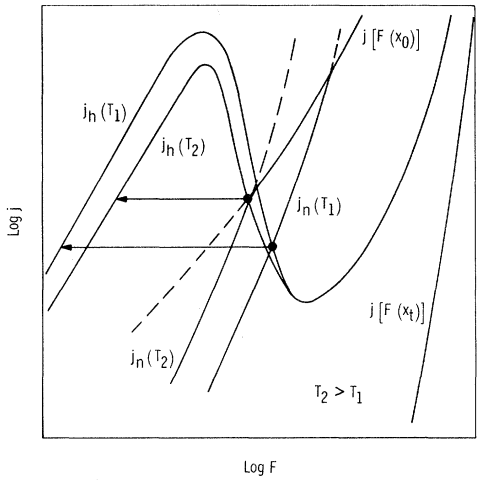

FIG. 5. $j_h(F)$ and $j_n(F)$ for two temperatures. $j[F(x_t)]$ and $j[F(x_0)]$ are also given and do not markedly depend on temperatures.

causes the field in the bulk and therefore the current through the crystal, to decrease, since the current in the bulk is exclusively given by drift.

As a result of this, the barrier will be further depleted and widened. An increased positive space charge is produced there to create and sustain the increased field (Fig. 6, curves 2 and 3). With the depletion of conductive electrons, a depletion of trapped electrons in this region must follow, with a time constant τ characteristic for ionization of filled traps of

$$\tau = (1/\alpha^*)\, e^{(E_c - E_{Fn})/kT}\,, \tag{14}$$

where α^* is the frequency factor (typically 10^{12} sec^{-1}) of the traps at the quasi-Fermi level E_{F_n}. This trap depletion causes the positive space charge and the field in the barrier region to increase further. The current through the crystal, therefore, must continue to decrease.

If the barrier height is not much larger than the distance of the quasi-Fermi level for electrons from the conduction band, the before-mentioned process may stop before the field in the barrier region reaches values in the field ionization range. The stationary current is then reached being sustained even at the density minimum in the barrier region by "drift." However, such a situation can only be achieved for very small applied voltages and very low barriers,[21] as evident from the continuity equation

$$F(x_m) = F_i n_i / n_m \tag{15}$$

(the index i refers to the crystal bulk).

In most occasions this is not the case, and the field in the barrier region will increase further, and field-enhanced ionization[14] may help to empty deeper traps more rapidly. The current through the crystal continues to decrease. This process must stop when all traps are ionized, i.e., when the maximum achievable positive space charge is reached.[22] If the maximum field in the barrier region is below the critical field for marked tunneling through the barrier, the barrier region must continue to widen, with most of the applied voltage drop across this region. Hence, the field in the remaining bulk approaches zero and the current through the crystal decreases to such a value as can be sustained via carrier leakage through the barrier (small amount of tunneling or thermal emission over the barrier).

However, if the density of defects in the band gap is sufficient to permit a positive space-charge layer of about 10^{13} cm^{-2}, the field in the barrier region can grow until it is large enough to allow for extensive tunneling. The current can stabilize at rather high densities and the voltage drop in the barrier region may amount to only a small fraction of the applied voltage V (for $V > 1$ V).

A. Space-Charge Creation Near the Cathode (Thermal Depletion of Traps)

The behavior discussed above can be described quantitatively in a somewhat simplified model by

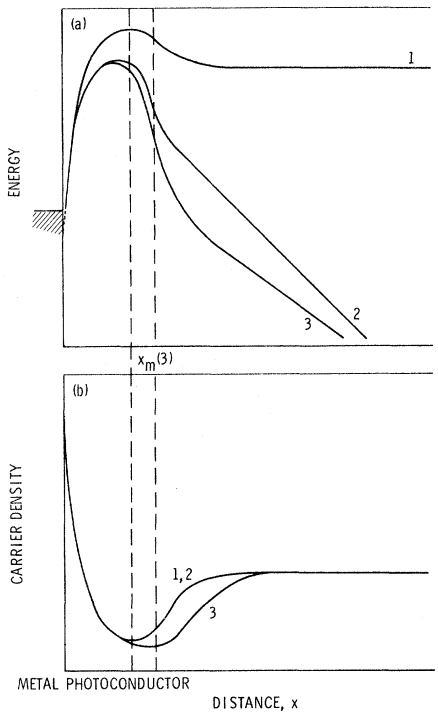

FIG. 6. Potential energy and carrier distribution vs distance from the interface: 1, without applied field; 2, immediately after an external field is applied; and 3, sometime thereafter.

analyzing the space-charge creation caused by electron redistribution in traps. This mechanism is probably the one observed in the kinetic analysis of Ref. 1. Assuming a trap distribution $N_t(E)$, of which $n_t(E)$ are filled, one approximates the space charge development as

$$\frac{\partial \rho(x,t)}{\partial t} = \int_{E_v}^{E_c} \frac{\partial n_t(E,x,t)}{\partial t}\, dE \tag{16}$$

(neglecting changes in the distribution of free carriers). From kinetic arguments one obtains

$$\rho(x,t) = \int_0^t dt' \int_{E_v}^{E_c} \{\alpha(E)\, n_t(E,x,t) - \beta(E)\, n(x,t) \times [N_t(E) - n_t(E,x,t)]\}\, dE \ , \tag{17a}$$

with $\alpha(E)$ the ionization probability and $\beta(E) = v_e q(E)$ the capture coefficient of traps (being a product of the velocity of electrons and the capture cross section). From detailed balance,

$$\rho(x,t) = \int_0^t dt' \Big| \int_{E_v}^{E_{F_n}} \beta(E)\, N_t(E) \times e^{(E-E_{F_n})/kT} [n_0 - n(x,t)]\, dE + \int_{E_{F_n}}^{E_c} \beta(E)\, N_t(E)\, [n_0 - n(x,t)] \Big| dE \ , \tag{17b}$$

with $n_0 = N_c \exp[-(E_c - E_{F_n})/kT]$ and traps below the quasi-Fermi level assumed to be filled before voltage was applied.

The change in field distribution in the barrier region is given by

$$F(x,t) = F(0,t) - (e/\epsilon\epsilon_0) \int_0^x \rho(x',t)\, dx' \ . \tag{18a}$$

Using the fact that $\int_0^L F(x,t)\, dx = V$, and that the applied voltage is time independent, and introducing $x_s(t)$, where for $x > x_s$ all parameters are space independent and $\rho = 0$, one obtains

$$F(0,t) = \frac{V}{L} + \frac{e}{\epsilon\epsilon_0 L} \int_0^L \int_0^x \rho(x't)\, dx'\, dx. \tag{18b}$$

Since in the space-charge region $n(x)$ is much smaller than n_0, one may approximate the integral in Eq. (18b) by $\rho(t)\, x_s(t)\, (1 - x_s/2L)$, and using Eq. (18a), one obtains

$$F(x_s,t) = \frac{V}{L} - \frac{e}{\epsilon\epsilon_0}\, \rho(t)\, \frac{[x_s(t)]^2}{2L} \ . \tag{19}$$

This is the field in the crystal bulk which gives the time-dependent current

$$j(t) = e\mu n_0\, F(x_s,t) \ . \tag{20a}$$

The time-dependence of the space-charge region can be obtained from current continuity by comparing the current generated in the space-charge region with that in the bulk:

$$e\, \frac{\partial \rho(t)}{\partial t}\, x_s(t) = e\mu n_0\, F(x_s,t) \ , \tag{20b}$$

yielding [from Eq. (19)]

$$F^2(x_s,t) + K(t)\, [F(x_s,t) - V/L] = 0 \ , \tag{21a}$$

with

$$K(t) = \frac{2\epsilon\epsilon_0 L}{e\mu^2 n_0^2\, \rho(t)} \left(\frac{\partial \rho(t)}{\partial t}\right)^2 \ . \tag{21b}$$

The distance $x_s(t)$ can be obtained from Eq. (20a), yielding

$$x_s^2(t) + \frac{K(t)\, \mu^2 n_0^2}{[\partial \rho(t)/\partial t]^2} \left[\frac{\partial \rho(t)}{\partial t}\, \frac{x_s(t)}{\mu n_0} + \frac{V}{L}\right] = 0. \tag{21c}$$

For very short times after the voltage is applied, $K(t)$ is very large ($\gg V/L$) and one obtains from Eq. (21a)

$$F(x_s,t) \simeq V/L \ , \tag{22a}$$

and from Eq. (21c)

$$x_s(t) \simeq \mu n_0\, V/L\, \frac{\partial \rho(t)}{\partial t} \ ; \tag{22b}$$

i.e., the field in the bulk, and therefore the current, remain essentially constant and the depleted region $x_s(t)$ grows [as $\partial\rho(t)/\partial t$ decreases[23]], in order to provide the current [see Eq. (20b)]. As the time increases, the growth of $\rho(t)$ and the decrease of $\partial\rho(t)/\partial t$ force the decrease of $K(t)$. When $K(t)$ has decreased far below V/L, which seemes to be fulfilled experimentally[24] for the cases discussed in Ref. 1, one obtains from Eq. (21a)

$$F(x_s,t) \simeq [K(t)(V/L)]^{1/2} \ . \tag{22c}$$

Hence [using Eqs. (20a), (20b), (21b), and (22c)] one sees that the current

$$j(t) \simeq e\, \frac{\partial \rho(t)}{\partial t}\, \left(\frac{2\epsilon\epsilon_0 V}{e\rho(t)}\right)^{1/2} \tag{23}$$

then decreases,[25] and the external field at the boundary

$$F(0,t) \simeq \frac{V}{L} + \left(\frac{2e}{\epsilon\epsilon_0}\, \rho(t)\, V\right)^{1/2} \tag{24}$$

increases monotonically in time, since $\rho(t)$ increases and $\partial\rho/\partial t$ decreases in time[23] as it becomes more difficult to ionize deeper and deeper traps with progressing depletion. It should be noted that with continuing depletion of deeper traps, the space-charge region contracts (see Fig. 7), since under these conditions

$$x_s(t) \simeq [2\epsilon\epsilon_0 V/e\rho(t)]^{1/2} \ . \tag{25}$$

This is because as more space charge is created in the barrier region with the field there increasing, the field in the bulk must decrease as the applied voltage is kept constant (Fig. 8). Although the thickness of the space-charge layer decreases, the space-charge density increases more rapidly causing the product $\rho(t)\, x_s(t)$, and thus the field at the boundary, to increase [see Eq. (24) and Fig. 8].

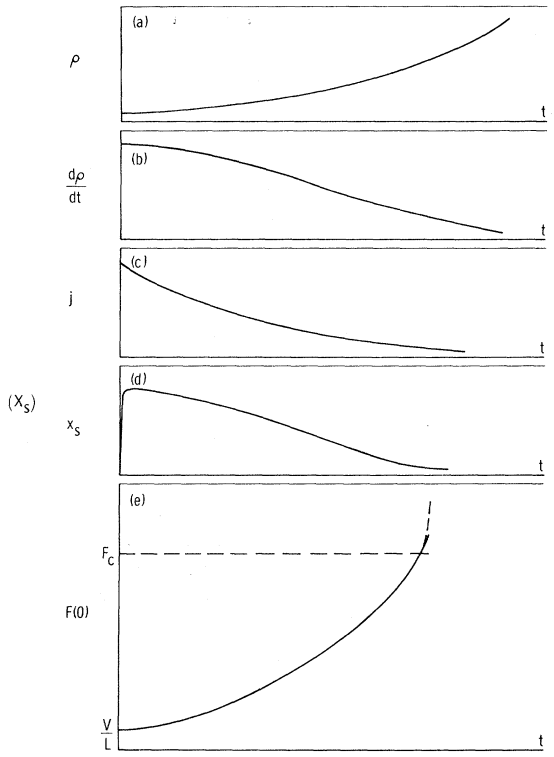

FIG. 7. Space charge $\rho(t)$, change of space charge $d\rho/dt$, current density j, space-charge region thickness x_s, and external field at the metal-photoconductor boundary $F(0)$, as a function of elapsed time after switching on the applied voltage.

B. Space-Charge Creation Near the Cathode (Field-Enhanced Depletion of Traps)

When the field at the boundary [Eq. (24)] exceeds the critical field for field-enhanced ionization, a very rapid ionization of deep traps sets in, causing the space charge and the field to increase in this region, and resulting in further acceleration of the trap ionization. It therefore seems justified to approximate this process by a step-mechanism, assuming that below a threshold field ($F < F_c$) no field ionization takes place, and that above F_c, ionization of the Coulomb-attractive deep trap level occurs. If x_1 is the position at which $F(x_1, t) = F_c$ and $\rho_1(t)$ is the ("saturation") space-charge density in the region $0 < x < x_1$, one obtains by proper replacements in Eq. (18a) and integrations:

$$V = [F_c - (e/\epsilon\epsilon_0)\rho(t)\, x_s'(t)]\, L + (e/\epsilon\epsilon_0)\{\rho(t)\tfrac{1}{2}[x_s'(t)]^2 + \rho(t)\, x_s'(t)\, x_1(t) + \rho_1(t)\tfrac{1}{2}[x_1(t)]^2\}\,, \quad (26)$$

where now $x_s'(t)$ is the width of the low-field ($F < F_c$) space-charge region. For the field in the bulk [hence for the current—see Eq. (20a)] one consequently obtains

$$F(x_0, t) = F_c - (e/\epsilon\epsilon_0)\rho(t)\, x_s'(t)\,. \quad (27)$$

On the other hand, the current is determined in the transient region by the sum of the two particle currents stemming from the regions $0 < x < x_1$ and $x_1 < x < x_1 + x_s'$:

$$j(t) = j_n(x_1, t) + e\,\frac{\partial\rho(t)}{\partial t}\, x_s'(t)\,, \quad (28)$$

with $j_n(x_1, t) = e(\partial\rho_1(t)/\partial t)\, x_1(t)$. Hence replacing $x_s'(t)$ in Eq. (27) from Eqs. (20a) and (28), one obtains

$$j(t) = e\mu n_0 F(x_s', t)$$

$$= e\mu n_0\, \frac{F_c + (1/\epsilon\epsilon_0)\rho(t) j_n(x_1, t)[\partial\rho(t)/\partial t]^{-1}}{1 + (e/\epsilon\epsilon_0)\mu n_0 \rho(t)[\partial\rho(t)/\partial t]^{-1}} \quad (29a)$$

and, for the distance $x_s'(t)$, it follows that

$$x_s'(t) = \frac{F_c - j_n(x_1, t)/e\mu n_0}{[\partial\rho(t)/\partial t]/\mu n_0 + (e/\epsilon\epsilon_0)\rho(t)}\,. \quad (29b)$$

This implies that at this time, $F(x_s', t)$ has decreased to a value which is small compared to V/L (the current has decreased considerably from its initial value); hence [from Eqs. (27) and (26)] one obtains—instead of Eq. (26)—

$$V \simeq (e/\epsilon\epsilon_0)\{\rho(t)\tfrac{1}{2}[x_s'(t)]^2 + \rho(t)\, x_s'(t)\, x_1(t) + \rho_1(t)\tfrac{1}{2}[x_1(t)]^2\}\,, \quad (26a)$$

which implies that as $x_s'(t)$ decreases, $x_1(t)$, and therefore $j_n(x_1, t)$ [see Eq. (29b)], must increase.[26]

The increase of $j_n(x_1, t)$ and of $\rho(t)\,[\partial\rho(t)/\partial t]^{-1}$ with t, forces $\rho(t)\, x_s'(t)$ to decrease, and hence, $F(x_s', t)$

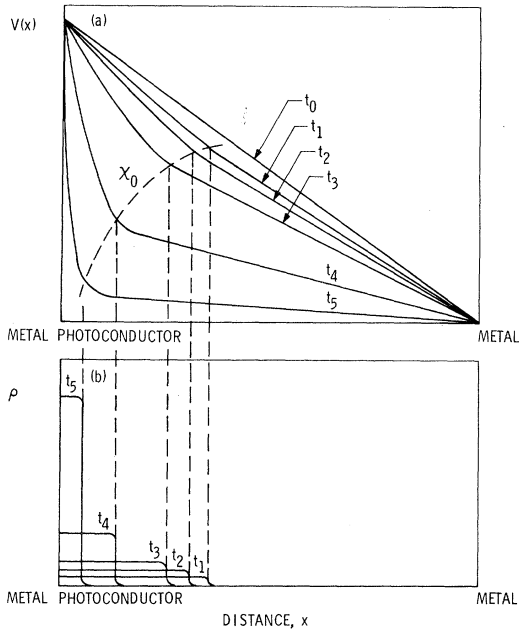

FIG. 8. (a) Simplified potential distribution and (b) space-charge distribution at different times $t_1 \ldots t_5$ after switching on the applied voltage (at t_0).

and therefore $j(t)$ to increase, during this time interval.[27] The increase in $j(t)$ will be maintained as long as $x_1(t)$ increases, i.e., as long as Eq. (26a) holds.

This process will terminate when total depletion of the field ionized centers is achieved. Then a new region of constant charge density $\rho_{1\,max}$ is created and will spread from the cathode. Now $x_1(t)$, the width of the region from which the current is generated, hence the current, will start to decrease again. The kinetic of these processes is pictured in Fig. 9. The field reaches its critical value "at" the cathode at t_1 and increases[28] while the width $x_s'(t)$ decreases as $x_1(t)$ increases (t_2 to t_4). Finally, a totally depleted region is created and $x_1(t)$ also decreases (t_5). The field "at" the cathode continues to increase monotonically while the current (see field in the bulk in Fig. 9) has decreased through a minimum (t_2, t_3), increased (t_4), and decreased again (t_5).

C. Onset of Tunneling Through the Barrier

As the monotonically increasing field at the cathode reaches another critical value,[8,9] tunneling through the barrier starts, and an equation similar to Eq. (28) with j_{tunn} instead of $j_n(x_1, t)$ determines the current through the crystal. The current therefore increases again as long as $\partial\rho/\partial t \neq 0$, until final stationarity is reached while the region where the

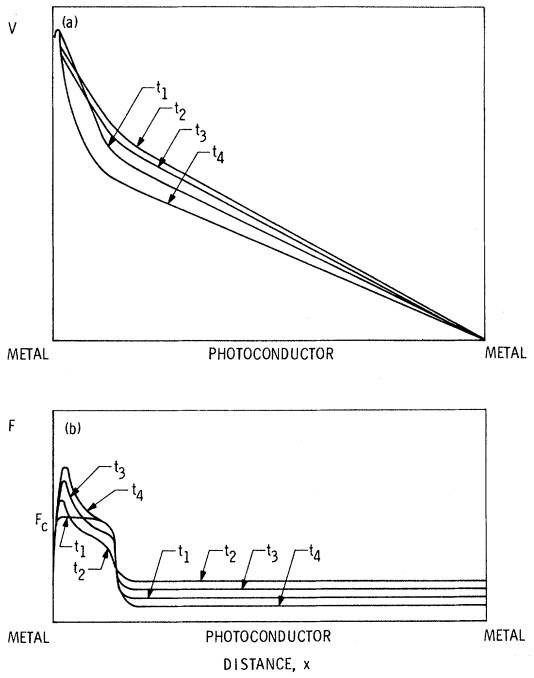

FIG. 9. (a) Potential and (b) field distribution at successive times $t_1 \ldots t_5$ after the critical field F_c for field-enhanced ionization is reached. See text.

current was previously generated vanishes due to partial trapping of electrons provided by the contact. (For this discussion the hole current is neglected since the measured gain factor is much larger than 1.)

Small fluctuations from this equilibrium of such current will be counteracted by either enhanced tunneling and recombination or by enhanced space-charge generation (as tunneling and recombination decrease).

In summary, it is expected that after applying a sufficiently large[29] voltage, the current should first decrease from an initially very high value representing drift in an essentially homogeneous external field $F_a = V/L$. This decrease is determined by thermal ionization of traps in the space-charge region of the blocking contact. If there is no other process generating current (except minority carrier currents which are neglected in this paper since they may predominate only at gain factors less than 1), the current should monotonically decrease to the low limit of diffusion over the barrier (perfectly blocking contact). Only if a current-generating mechanism is unveiled as the field close to the cathode increases, can a minimum occur in the transient. In the present case it is suggested that, as the field near the cathode starts to exceed values at which field ionization of defects becomes marked, e.g., via field-enhanced ionization of electrons from Coulomb attractive traps, an increase of the current may occur until these traps are depleted. As the high-field region close to the cathode widens, the current should decrease again until tunneling through the barrier starts. Then the current must again increase, as self-stabilization occurs via recombination of some of the tunneling electrons with empty traps in the space-charge region (see Sec. III). Such nonmonotonic behavior is indeed observed.[1]

When stationarity is approached, the positive space-charge region must terminate rather abruptly near x_0, since with increasing distance from the cathode the tunneling electrons become increasingly thermalized, that is, the reaction kinetics determining the space charge behaves increasingly bulklike. However, as mentioned in Sec. III, the space charge tends to turn negative for fields exceeding the field of the cathode-adjacent high-field domain (as, e.g., in the $F_{II} \rightarrow F_{III}$ transition), exerting a strong compensating tendency on the positive space charge closer to the electrode (see Fig. 10).

Two current minima can be well distinguished at low optical excitation (Figs. 9 of Ref. 1). From the intermediate current maximum, one can estimate the density of electrons released from deep traps by field ionization:

$$n_t = (1/ebwx_1) \int_{peak} i\,dt \ , \qquad (30)$$

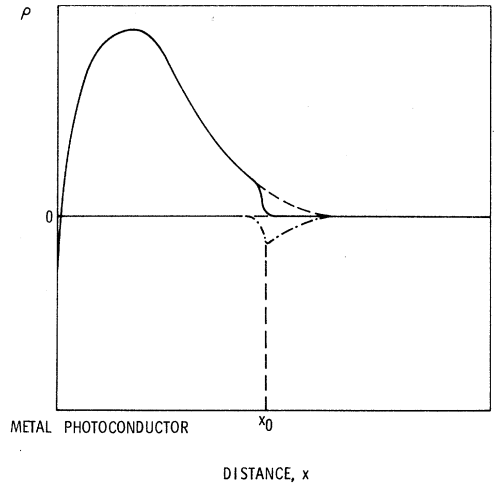

FIG. 10. Space-charge distribution near a blocking cathode. The dash-dotted curve indicates the negative space-charge fraction created near x_0 which aids to reduce the total space charge rapidly at $x = x_0$.

with b the thickness and w the width of the crystal. From Fig. 9(a) in Ref. 1, one obtains for the additional particle current $\int i\,dt \simeq 5\times10^{-10}$ A sec. Hence, with a cross section of the crystal of $\sim 3 \times 10^{-3}$ cm^2, additionally released electrons cause a space-charge layer density of $\sim 10^{13}$ cm^{-2} which is sufficient to create a field of $\sim 10^6$ V/cm and initiate tunneling.

With increased optical excitation, the quasi-Fermi level is shifted closer to the conduction band and thermal depletion of traps is increased. Thus, a space-charge layer sufficient to create a field F_c can be formed more quickly, making the intermediate maximum occur at a shorter time in agreement with the experimental observation.[1]

With further increased optical excitation, the first current minimum is not resolved, and may actually disappear as thermal release competes more favorably with field ionization. However, the second minimum can be followed over a wide range of excitation densities and shifts nearly linearly towards shorter times with increasing excitation. Such behavior can be expected since the stabilizing recombination of tunneling electrons will occur sooner when more shallow traps are available for carrier redistribution at higher optical excitation. The time constant for this redistribution is expected to be of the order of typical redistribution times of electrons near the Fermi level (traps above E_F remain depleted), also in agreement with observation.

However, the kinetics are too complex to encourage a detailed quantitative analysis at this time. It may suffice in the realm of this paper to show qualitative agreement with the experiment to indicate that the proposed model may explain the electronic behavior of the space charge region near a blocking contact on photoconducting CdS.

VII. SUMMARY

In photoconductive CdS the current through the crystal is markedly influenced by blocking contacts and is dependent on the type of contact metal. At higher current densities this behavior is independent of typical interlayers of absorbed gases. At sufficient applied voltages, the observed current densities are many orders of magnitude higher than the thermal-emission saturation current over the barrier. (The barrier height can be easily determined in the zero-current limit.[2])

It seems plausible, therefore, to assume that tunneling through the barrier is the process responsible for current continuity at high current densities. (Since the gain factor is larger than one, a hole current cannot be responsible.) On the other hand, the observed fields in the bulk of the CdS (using a high-field domain analysis) are far below the critical field for tunneling. This field cannot increase when approaching the cathode (as evidenced by the field of directions) as long as the Poisson and simple transport equations are valid. This leaves only a slab of a width of a few mean free paths ($\sim 6\times10^{-6}$ cm) to build up a positive space charge sufficient to increase the field to at least a value necessary for tunneling of 3×10^5 V/cm. This requires a level density of about 10^{18} cm^{-3} for storage of the space charge, which is at least one order of magnitude larger than the level density observed in the energy range accessible to conventional experimental observation. Since storage of a sufficient density of positive space charge can only be envisaged in levels in the band gap (Sec. II), this leaves only one possibility to explain the observed behavior within the frame of known effects: namely, to assume that close to the (dark) Fermi level in CdS, there exist donor levels produced by intrinsic defects of at least 10^{18} cm^{-3} density. (Cadmium interstitials or sulfur vacancies are suggested as the native defect responsible for the level near 0.8 eV below the conduction band.) This may account for the fact that CdS is not observed to be p type under equilibrium doping conditions.

The presence of these high-density deep levels with field-dependent kinetic coefficients is further substantiated by the transient behavior of the current. The formation of this space-charge layer is caused by carrier depletion in an external field, but can be maintained only by the specific recombination kinetics in the barrier region probably caused by the highly anisotropic momentum distribution[10,11] of tunneling electrons. This is evidenced by the fact that in the crystal bulk, a negative (rather than a positive) space charge is formed

when the field increases into the 10^5 V/cm range (as observed in the transition range of anode-adjacent high-field domains[17]).

The boundary conditions for the solution of the Poisson and the transport equations are uniquely determined at the bulk boundary of the above mentioned slab (i.e., at x_0) by the interplay between tunneling and carrier thermalization and recombination in this slab. Since the thickness of the slab is nearly independent of doping (as long as the mean free path is), the carrier density and the field at x_0 are determined by the barrier height and the ability to store space charge in the region $x < x_0$. One concludes that $F(x_0)$ will be smaller and $n(x_0)$ larger, the higher the density of donors in the slab and the lower the barrier height (work function between metal and CdS). For a sufficiently high donor density within the slab, the individuality of the metal will disappear with respect to the electrical properties of the entire crystal as is observed for highly disordered CdS.[20] The contact in the latter case will have injecting characteristics. It is further suggested that in materials where the individuality of the metal does not show, such high density of deep native donors is always present[30] (e.g., CdSe). On the other hand, it is expected that materials which have a much lower density of levels useful for storage of the proper space charge should show a thermionic-saturation current behavior for majority carriers.

The proposed model is in qualitative agreement with all observed experimental facts.[1] However, it is too early for a quantitative analysis of the reaction kinetic behavior in the space-charge region, since the critical parameters, as e.g., anisotropy of the momentum distribution of tunneling electrons, the energy-dependent capture cross sections, the energy and density of donor levels, and the scattering parameters in the space-charge region are presently not sufficiently known.

ACKNOWLEDGMENTS

It is a pleasure for us to acknowledge very helpful discussion with Professor H. Kallmann and Professor C. A. Mead in the early phase of this work. Critical discussions with Dr. P. Massicot are gratefully acknowledged.

---

*This paper presents the results of one phase of research sponsored by the National Aeronautics and Space Administration under Contract No. NAS7-100 and the U.S. Office of Naval Research, Washington, D.C.

†Present address: Comisión Nacional de Energie Atómica, Buenos Aires, Argentina.

[1]R. J. Stirn, K. W. Böer, and G. A. Dussel, preceding paper, Phys. Rev. B **7**, 1443 (1973).

[2]W. Ruppel, in *Semiconductors and Semimetals*, edited by R. K. Willardson and A. C. Beer (Academic, New York, 1970), Vol. 6.

[3]K. W. Böer and P. Voss, Phys. Rev. **171,** 899 (1968).

[4]K. W. Böer, Phys. Status Solidi A **3,** 1007 (1970).

[5]C. A. Mead, Solid-State Electron. **9,** 1023 (1966).

[6]K. W. Böer, G. A. Dussel, and P. Voss, in *Ohmic Contacts to Semiconductors,* edited by B. Schwartz (The Electrochemical Society, New York, 1969).

[7]K. W. Böer, G. A. Dussel, and P. Voss, Phys. Rev. **179,** 703 (1969).

[8]G. H. Parker and C. A. Mead, Appl. Phys. Lett. **14,** 21 (1969).

[9]G. H. Parker and C. A. Mead, Phys. Rev. **184,** 780 (1969).

[10]C. B. Duke, in *Tunneling Phenomena in Solids*, edited by E. Burstein and S. Lundquist (Pergamon, New York, 1969), p. 31.

[11]R. Stratton, in Ref. 10, p. 105.

[12]Taking into consideration field heating of carriers.

[13]With $\Delta x_{\max}\rho_{\min}=3\times10^{12}$, it follows that $\rho_{\min}\simeq10^{17}$ cm, which is at least one order of magnitude larger than $N_t(0.7\leq E_c-E_t\leq0.3$ eV) (see Ref. 1).

[14]G. A. Dussel and K. W. Böer, Phys. Status Solidi **39,** 375 (1970).

[15]G. A. Dussel and K. W. Bóer, Phys. Status Solidi **39,** 391 (1970).

[16]Diffusion doping does not shift the Fermi level to lower values.

[17]K. W. Böer and P. Voss, Phys. Status Solidi **28,** 355 (1968).

[18]Other capture mechanisms depend to a much lesser extent on the electron energy.

[19]In the bulk the electron capture obviously predominates, essentially filling these centers and some traps at $E_c-E_t<0.8$ eV. These filled traps are less numerous causing a net negative space charge with much smaller density, hence, a considerably wider field transition range (domain wall 10^{-3} cm) as experimentally observed (Ref. 17).

[20]J. Fassbender, Z. Phys. **145,** 310 (1953).

[21]Aside from the continuity-equation condition, the barrier has to be wide enough to allow for drift near x_m.

[22]In actual practice the transport and redistribution of minority carriers cannot be neglected. We will return to this point later in this paper.

[23]Assuming an exponential depletion of traps, i.e., $\rho(t)=\rho_0\times[1-\exp(-t/\tau)]$, one obtains $\partial\rho(t)/\partial t=(\rho_0/\tau)\exp(-t/\tau)$, which decreases with increasing time. The decrease of the rate of charge formation with increasing time is quite general, for any assumed trap distribution.

[24]The current has decreased to a small fraction of its initial value when voltage is applied.

[25]The critical time when the current starts to decrease is determined by $K(t)=V/L$ and, for exponential trap depletion, can be expressed as $t_0=\tau\ln[(\tau/\tau_r)]\,(V/LF^*)^{1/2}$ for $(\tau/\tau_r)\times(V/LF^*)^{1/2}\ll1$ and $t_0=\tau_r(\tau_r/\tau)\,(L/V)F^*$ for $(\tau/\tau_r)(V/LF^*)^{1/2}\gg1$, with $\tau_r=\epsilon\epsilon_0/e\mu n_0$ and $F^*=(e/\epsilon\epsilon_0)\rho_0 L$. Hence τ_0 is of the order of the dielectric relaxation time (since τ is limited by τ_r) and, in the investigated case, is of the order of 10^{-7} sec.

[26]This can be seen by writing $\rho_1(t)=\rho_F(t)$, where $\rho_F(t)$ is the field induced part of the space charge. Equation (26a) can now be rewritten as $V\simeq(e/\epsilon\epsilon_0)[\rho(t)(x'_s+x_1)^2/2+\rho_F x_1^2/2]$. For times shortly after $F(0,t)=F_c$, the relation $\rho_F(t)\ll\rho(t)$ holds and x'_s+x_1 must decrease as $\rho(t)$ increases [see also Eq. (25)]. For times such that $(e/\epsilon\epsilon_0)\mu n_0\rho(t)/(\partial\rho(t)/\partial t)\lesssim1$, one concludes from Eq. (29a) that $x'_s(t)$ must decrease since $x'_s(t)\rho(t)$ increases slowly while $\rho(t)$ increases much faster. Therefore $x_1(t)$ must increase.

[27]Note that $x'_s(t)$ is influenced very little by $j_n(x_1,t)$ [see Eq. (29a)] since $j_n(x_1,t)\ll e\mu n_0 F_c$, while $j_n(x_1,t)$ can greatly affect $F(x'_s,t)$ and therefore the current [see Eq. (29)]

since $(1/\epsilon\epsilon_0)\rho(t)/(\partial\rho(t)/\partial t) \gg 1/e\mu n_0$.

[28]The field at the cathode increases as long as the total space-charge density $\rho\Delta x$ increases. This is assured even though the voltage drop in the space-charge region $[\sim\rho(\Delta x)^2]$ decreases as long as ρ increases more than Δx decreases (see Sec. VI B).

[29]To finally allow for tunneling.

[30]The assumption of surface states for a "pinning of boundary condition" in such materials seems to be misleading.

PHYSICAL REVIEW B VOLUME 7, NUMBER 4 15 FEBRUARY 1973

Resistivity and "One Dimensionality" in Ti_2O_3[†]

L. L. Van Zandt and P. C. Eklund
Department of Physics, Purdue University, Lafayette, Indiana 47907
(Received 6 April 1972)

Energy bands in a Ti_2O_3 lattice are parametrized in terms of overlap matrix elements. The requirements of "one-dimensional" energy bands as an explanation for recently observed specific-heat anomalies are compared to this parametrization and shown to be in conflict by three orders of magnitude. Resistivity measurements on oriented samples are also shown and also fail to support the "one-dimensional" hypothesis.

Sjöstrand and Keesom[1] have recently observed anomalous low-temperature specific heats in samples of Ti_2O_3 doped with a few percent V_2O_3. They tentatively ascribe the anomalous behavior to the presence of holes introduced by the V ions into a "one-dimensional" valence band of the host material with a single low mass direction parallel to the axis. Briefly, the density of electronic states varies in proportion to $E^{1/2}$ in a three-dimensional structure but like $E^{-1/2}$ in a one-dimensional array, where E is the single-electron (or hole) energy as measured from the band edge. The singularity in $E^{-1/2}$ near the band edge provides an enormous density of states for dopant-introduced carriers and so has been proposed to fit the anomalies as observed.

The purpose of this communication is to report resistivity measurements whose interpretation appears to conflict with one dimensionality in the electronic structure and to consider and emphasize the unavoidable implications of one dimensionality, which would suggest that the hypothesis should be accepted only with reluctance.

In considering the implications of the one-dimensional hypothesis, we need to consider the question of the direction of that one dimension, that is, which of the three crystal dimensions is the favored one. Ti_2O_3, with and without vanadium, crystallizes in the corundum structure of symmetry D_{3d}. The structure thus includes a preferred direction, the c axis. To avoid breaking the symmetry, therefore, the favored direction should be the c axis, or there should be three degenerate sets of electronic states with favored directions symmetrically arranged. Both alternatives encounter difficulties when the actual lattice structure is considered, however, as will be seen.

The crystal binding in Ti_2O_3 is strongly ionic in character; three of the 22 electrons of a neutral Ti atom are transferred to oxygen sites, leaving a single d electron on the Ti^{3+} ion. In a rhombohedral field, the five orbital atomic d states are split into two pairs of doubly degenerate e_g states and a single nondegenerate a_{1g} state. That pure Ti_2O_3 is an insulator indicates that the a_{1g} state lies lowest,[3,4] and it is the bands formed from this state that we shall study for one dimensionality.

We shall work in the tight-binding approximation, but since there are several Ti atoms in a unit cell, the calculation is somewhat more complicated than the usual textbook case.

When the atoms are brought together to form molecules, the atomic wave functions overlap and the atomic levels are split into molecular levels. Bringing the molecules together to form a crystal finely splits, or broadens, the molecular levels into bands.

We can simplify somewhat by an approximation in which we treat the individual Ti_2O_3 molecules as identical although in fact there are two sets of molecules related by a glide reflection. The long distance between inequivalent molecules of the same unit cell in the actual structure makes this a slight approximation and one which certainly does not qualitatively change our conclusions.

Ti_2O_3 molecules are located on the vertices of a rhombohedral lattice described by lattice vectors as in Table I, which also relates them to the crystal parameters c and a.

In zeroth order, each Ti site affords one a_{1g} atomic function $\chi_a(\vec{r}-\vec{r}_i)$. The one-electron Hamiltonian is

$$H = -\frac{\hbar^2}{2m}\vec{\nabla}^2 + \sum_i v(\vec{r}-\vec{r}_i)\,, \tag{1}$$

where $\vec{r}_i$ runs over all the Ti ions. We first construct a molecular wave function,

$$\chi_m(\vec{r}) = a_1\chi_a(\vec{r}-\tfrac{1}{2}d\hat{z}) + a_2\chi_a(\vec{r}+\tfrac{1}{2}d\hat{z})\,; \tag{2}$$